

Design, Synthesis, and Evaluation of Tetrahydropyrrolo[1,2-*c*]pyrimidines as Capsid Assembly Inhibitors for HBV Treatment

Xiaolin Li,[†] Kai Zhou,[†] Haiying He,^{*,†} Qiong Zhou,[†] Ya Sun,[†] Lijuan Hou,[†] Liang Shen,[†] Xiaofei Wang,[†] Yuedong Zhou,[†] Zhen Gong,[†] Shibo He,[†] Huangtao Jin,[†] Zhengxian Gu,[†] Shuyong Zhao,[‡] Long Zhang,[‡] Chunyan Sun,[‡] Shansong Zheng,[‡] Zhe Cheng,[‡] Yidong Zhu,[‡] Minghui Zhang,[‡] Jian Li,[†] and Shuhui Chen[†]

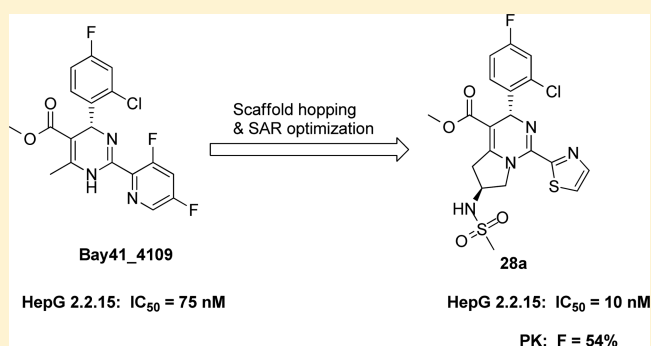
[†]WuXi AppTec (Shanghai) Co., Ltd., 288 FuTe Zhong Road, Shanghai 200131, P. R. China

[‡]Shandong Provincial Key Laboratory of Small Molecular Targeted Drugs, Qilu Pharmaceutical Co., Ltd., No. 243 Gong Ye Bei Road, Jinan, Shandong Province 250100, P. R. China

S Supporting Information

ABSTRACT: The discovery of novel tetrahydropyrrolo[1,2-*c*]pyrimidines derivatives from Bay41_4109 as hepatitis B virus (HBV) inhibitors is herein reported. The structure–activity relationship optimization led to one highly efficacious compound **28a** (IC₅₀ = 10 nM) with good PK profiles and the favorite L/P ratio. The hydrodynamic injection model in mice clearly demonstrated the efficacy of **28a** against HBV replication.

KEYWORDS: Hepatitis B virus (HBV), tetrahydropyrrolo[1,2-*c*]pyrimidines, capsid assembly inhibitor

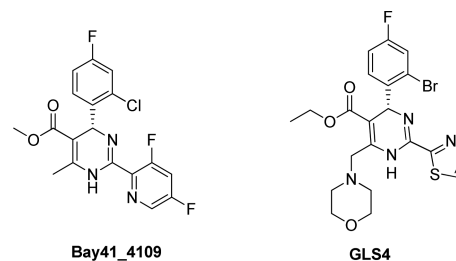


Hepatitis B is a potentially life-threatening liver disease caused by the hepatitis B virus (HBV) infection. Over 350 million people have chronic HBV infection.¹ Chronic HBV infection can lead to liver cirrhosis and hepatocellular carcinoma (HCC).² Currently, there are two types of anti-HBV agents in the market: immune modulators (IFN- α) and nucleoside(s) as reverse transcriptase inhibitors (Lamivudine, Entecavir, Telbivudine, Adefovir and Tenofovir).³ However, the usage of IFN- α is limited due to its low efficacy, high cost, and serious side effects; while nucleoside(s) often result in drug-resistance after long-term treatment.^{4,5} Moreover, both IFN- α and nucleoside(s) analogues cannot eradicate chronic HBV infection. Therefore, it is crucial to develop safer and more effective anti-HBV agents with novel mechanisms.^{6–8}

Heteroaryldihydropyrimidines (HAPs), discovered by a cell culture-based screening, were identified as a novel class of HBV inhibitors targeting capsid assembly and RNA packaging.⁹ It was reported that HAPs could enhance the rate of assembly and cause the formation of aberrant capsid, thus leading to decreased production of virions.¹⁰ However, HAPs were hydrophobic due to their special chemical structures.^{11,12} The poor water solubility significantly affected the drug candidate's oral PK properties and eventually limited the chance of being developed into a pharmaceutical product.

GLS4 (Scheme 1), derived from BAY41–4109 (Scheme 1), is currently in a phase II clinical trial as an anti-HBV agent,

Scheme 1. Chemical Structures of BAY41-4109 and GLS4



which also targets the HBV capsid formation.^{13–16} GLS4 was as potent as the prototype-BAY41–4109. Moreover, it can inhibit both wild-type and Adefovir resistant strains of HBV in cell culture. However, the poor oral bioavailability of GLS4 might become a hurdle for further development.

Received: July 18, 2017

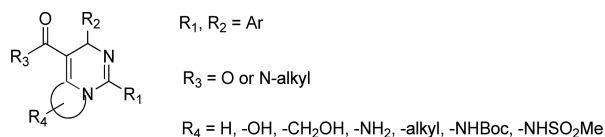
Accepted: August 24, 2017

Published: August 24, 2017

We herein report the approaches for the design, synthesis, and biological evaluation of a novel series of 3,5,6,7-tetrahydropyrrolo[1,2-*c*]pyrimidine derivatives as HBV capsid assembly inhibitors.

The derivatives (Scheme 2) were designed based on HAPs. Although it was reported that blocking the hydrogen on

Scheme 2. Chemical Structures of the Derivatives



pyrimidine with alkyl group resulted in loss of antiviral activity,^{17,18} we discovered that the fused ring analogues could maintain moderate to excellent potency.

The analogues in Table 1 were evaluated by the cell-based anti-HBV assay. The HepG2.2.15 cells were seeded at 4×10^4 cells/well in a 96-well plate (100 μL /well) in seeding medium

Table 1. Anti-HBV Activity of the Fused Ring Analogues in HepG 2.2.15 Cells

Compd No	Structure	^a IC ₅₀ (μM)
Bay41_4109		0.075
GLS4		0.012
1		4.1
2		0.30
3		1.4
4		2.5
5		9.3
6		3.5
7		0.77
8		0.81

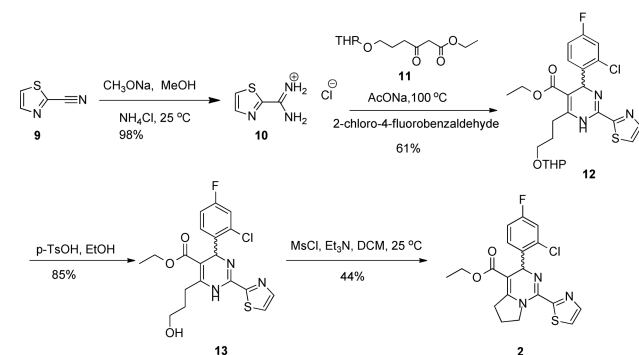
^aMean value of three experiments.

and incubated overnight at 37 °C in a 5% CO₂ humid atmosphere. The next day, compounds were added to the cell culture. Three days later, cells were replenished with fresh medium. After another three-day incubation, cell culture supernatants were collected and stored at -80 °C until HBV DNA was used. HBV DNA was extracted from supernatants with QIAamp 96 DNA Blood Kit and quantified by qPCR.

The IC₅₀ data in Table 1 showed the fused ring analogues can keep moderate activity. Among them, compound 2 possessed the best potency against HBV.

A general synthetic route for compound 2 is illustrated in Scheme 3. The THP protected ethyl 3-oxoheptanoate was

Scheme 3. Synthetic Route of 2

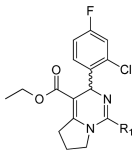


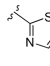
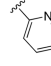
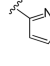
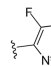
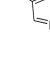
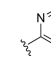
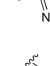
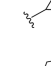
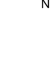

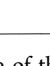
reacted with amidine 10 and the substituted benzaldehyde to produce the cyclized compound 12 under the Biginelli condition.¹⁹ Compound 12 was deprotected with *p*-TsOH to afford compound 13, followed by cyclization in the presence of MsCl/Et₃N to generate the racemic compound 2.

Utilizing the most potent compound 2 as a starting point, we first investigated the effects of different R₁ groups as shown in Table 2. The structure–activity relationship (SAR) analysis indicated that the thiazole group is the best moiety in this region.

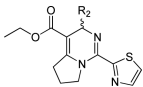
We explored the further SAR-based optimization of compound 2 at the R₂ position (Table 3). 2-Bromo-4-fluorophenyl (15a) provided a comparable activity (IC₅₀ = 0.21 μM). Replacement of the phenyl at 2, 3, or 4 position can retain the potency, such as 2-chloro-3-fluorophenyl (15b, IC₅₀ = 0.31 μM). However, it led to less potency if substituted at 2, 5 or 2, 6 positions, for example, 2-chloro-5-fluorophenyl (15c) and 2-chloro-6-fluorophenyl (15d). 2,4-Difluorophenyl (15e, IC₅₀ = 0.51 μM) and 3,4-difluorophenyl (15f, IC₅₀ = 0.43 μM) analogues maintained similar potency. No significant potency improvement was observed by introducing a methyl group at the 2-position of phenyl (15g, IC₅₀ = 0.45 μM). The replacement of 2-bromo-4-fluorophenyl with 1-methyl-1*H*-pyrazol-5-yl, resulted in the loss of potency, such as compound 15m or 15k. Besides, introduction of pyridine analogues (15i and 15j) at R₂ position also led to the loss of potency.

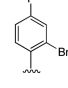
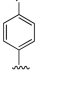
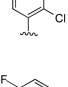
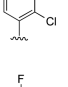
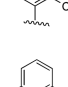
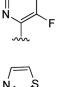
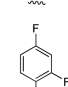
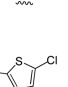
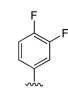
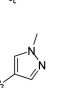
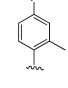

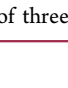
Based on the above result, further SAR was investigated at the R₃ region (Table 4). We found it led to loss of potency by replacing ethyl with 2-methoxyethyl carboxylate (16c) and 2-(dimethylamino)ethyl carboxylate (16d), but no difference if replaced with a methyl group (16a). The decline in potency was also observed when the ethyl group of 16a was replaced with the similar methoxymethyl group (16b) or 2,2-difluoroethyl group (16e). Furthermore, replacement of the

Table 2. Anti-HBV Activity in HepG2.2.15 Cells via R₁ Modification


Compd No	R ₁	* IC ₅₀ (μ M)	Compd No	R ₁	* IC ₅₀ (μ M)
2		0.3	14f		8.3
14a		2.8	14g		1.6
14b		>10	14h		>10
14c		2.0	14i		>10
14d		6.3	14j		>10
14e		>10			

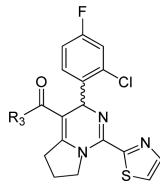
*Mean value of three experiments.

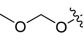
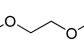
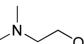
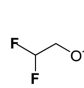
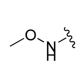
Table 3. Anti-HBV Activity in HepG2.2.15 Cells via R₂ Modification


Compd No	R ₂	* IC ₅₀ (μ M)	Compd No	R ₂	* IC ₅₀ (μ M)
15a		0.21	15h		1.2
15b		0.31	15i		>10
15c		>10	15j		>10
15d		>10	15k		>10
15e		0.51	15l		1.7
15f		0.43	15m		>10
15g		0.45			

*Mean value of three experiments.

ethyl carboxylate with a *N*-methoxy carboxylate (**16f**, IC₅₀ = 5.0 μM) did not maintain the potency.

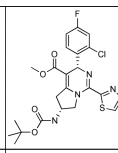
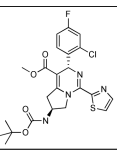
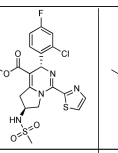
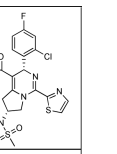
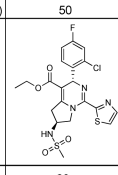
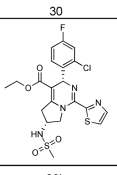
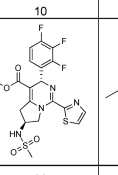
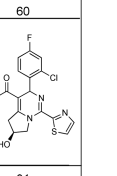
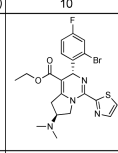
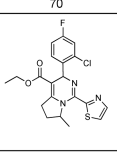
Table 4. Anti-HBV Activity in HepG2.2.15 Cells via R₃ Modification


Compd No	R ₃	* IC ₅₀ (μ M)
2	OEt	0.3
16a	OMe	0.32
16b		2.1
16c		>10
16d		>10
16e		2.0
16f		5.0

*Mean value of three experiments.

Interestingly, when we investigated the substituents at the five-membered ring, we found compounds **26** and **27** with a Boc group also showed good potency with IC₅₀ = 50 and 30 nM, respectively (Table 5). So we did further exploration at this region and identified that methylsulfonyl analogues such as **28a**, **29a**, and **30** possessed excellent activities. The absolute stereochemistry of **30** was determined by the single crystal X-

Table 5. Anti-HBV Activity in HepG2.2.15 Cells

Structure				
Cpd.	26	27	28a	28b
*IC ₅₀ (nM)	50	30	10	60
Structure				
Cpd.	29a	29b	30	31
*IC ₅₀ (nM)	10	70	10	320
Structure				
Cpd.	32	33		
*IC ₅₀ (nM)	500	8000		

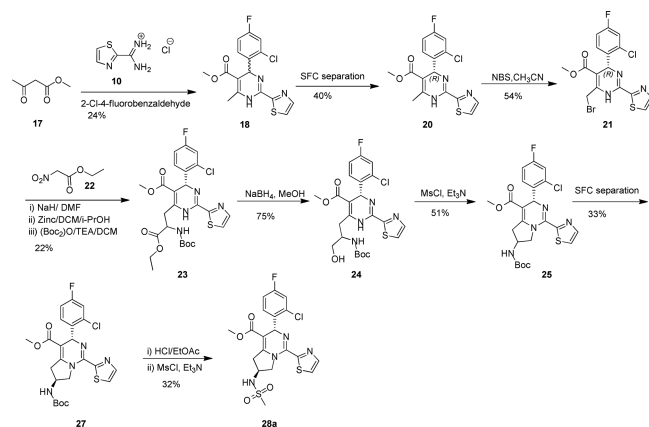
*Mean value of three experiments.

ray study (see Supporting Information). Compared to (3*R*,6*R*) isomers such as **28b** ($IC_{50} = 60$ nM) and **29b** ($IC_{50} = 70$ nM), the (3*R*,6*S*) isomers (**28a** and **29a**) were 6–7-fold more potent. Based on the efficacy of **28a** and **29a**, there was no difference if methyl ester replaced by ethyl ester. We kept the ethyl ester moiety and conducted the optimization on the pyrrolo ring, but hydroxyl (**31**), *N,N*-dimethyl (**32**), and methyl (**33**) analogues did not keep potency.

To gain deeper insights into the mechanisms of our compounds, we did the evaluation activity of **28a**, Bay41_4109, and GLS4 against HBV capsid assembly in the capsid quenching assay. Compounds **28a**, Bay41_4109, and GLS4 had IC_{50} values of 0.8, 0.43, and 1.2 μ M, respectively, which proved the similar capsid assembly inhibition mechanism.

A general synthetic route for compound **28a** is illustrated in Scheme 4. The compound **10** reacted with 2-Cl-4-F-

Scheme 4. Synthetic Route of 28a



benzaldehyde and ethyl 3-oxobutanoate (**17**) to generate the cyclized compound **18** under the Biginelli condition.¹ The enantiopure **20** was obtained through SFC chiral separation of the stereomixtures eluting with a mixed solvent of 85% supercritical CO_2 /15% EtOH at 100 mL/min rate. The absolute stereochemistry of (–)-enantiomer **20** was determined by its rotation value as reported.²⁰ Bromination of compound **20** generated **21**, which was reacted with **22** via three steps to give compound **23**. The subsequent reduction of **23** with $NaBH_4$ afforded compound **24**. Compound **25** was generated by cyclization of **24** in the presence of MsCl and Et_3N . The compounds **26** and **27** were separated by the of SFC separation with higher polarity of **27**. Compound **27** reacted with HCl/EtOAc to give the amine intermediate, then coupled with MsCl to generate compound **28a**.

Computer Modeling on Interaction of Compound 28a with HBV Capsid Protein. The dihydropyrimidine compounds can potentially bind to the interface of HBV core proteins, disrupting the formation of HBV capsid, therefore blocking the lifecycle of HBV.^{21–23} To better understand the SAR, some of the analogues in this work were docked into the crystal structure of HBV capsid (PDB code 5GMZ).

The binding pose of sulphonamide compound **28a** in the core protein is shown in Figure 1. The F- or Cl-phenyl occupies a compact and hydrophobic pocket, which consists of Thr33, Ile105, Leu30, Pro25, and Trp102 in one of the core proteins (chain B) and Val124, Arg127 and Thr128 in the other core protein (chain C). This pocket is very tight and hydrophobic,

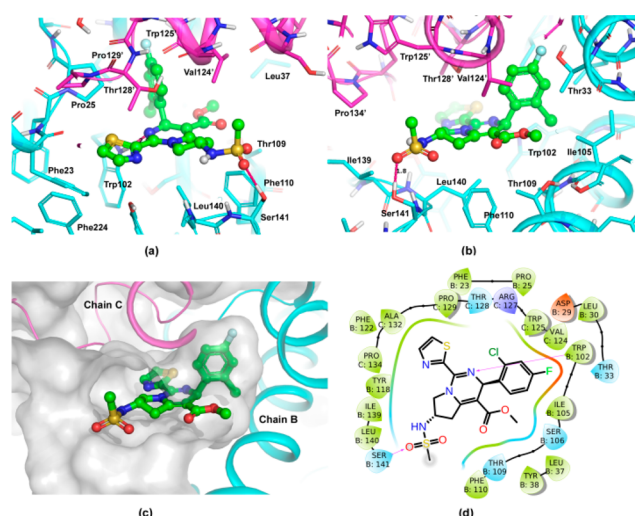


Figure 1. Putative binding pose of compound **28a** in HBV capsid. The core proteins, chains B and C, are shown in magenta and cyan cartoon. The ligand is shown as ball-and stick, where carbon atoms are in green. (a) View from the left-hand side of the entrance to binding site. (b) View from the right-hand side. (c) Binding pocket of the interface of core proteins. (d) Two-dimensional plot of compound **28a** in HBV capsid. The figures were prepared by Pymol²⁴ and Maestro²⁵ packages.

where the fluorine, chlorine, and bromine analogues are potent, but polar and bulky groups are generally not well tolerated (Table 3). The dihydropyrimidine can catch a key hydrogen bond to Trp102, as well as have hydrophobic interactions with Leu140 and Val124. However, the dihydropyrimidine core has a unique conformation, which facilitates the F-, Cl-phenyl binding to the tight pocket with an optimal dihedral angle. The thiazole can form hydrophobic interactions with Pro25 and Thr128, as well as π - π stacking with Phe23 and Tyr118. Some heterocycles with high polarity, such as pyrrolole and pyridine, can reduce activity. Moreover, saturated rings may even significantly drop in activity (Table 2). Most of these interactions lie in the deep pocket, stabilizing the conformation of **28a** in the interface of HBV core proteins.

The fused pyrrolidine can form hydrophobic interactions with Leu140, Phe110, and Val124, moreover, it acts as a rigid linker, which can deliver a hydrophilic tail to a region near solvent. Given the high lipophilicity of lead compound **2**, the free space around this region makes it possible to introduce hydrophilic groups to improve the solubility and pharmacokinetics properties. The vicinity of this hydrophilic region has Leu140 and Ser141, where two amides on main chain and a hydroxyl on side chain point to the inner pocket, forming a hydrogen bond donor rich region. The sulphonamide potentially can catch a hydrogen bond to Ser141, stabilizing the conformation of compound **28a** in the binding pocket (Figure 1). For the potent analogue **26**, its carbamate tail can also catch a hydrogen bond to Ser141, and its *t*-Bu can have additional hydrophobic interactions with Pro134 and Ile139. However, those compounds with less hydrogen bond acceptors on the tail (**31**, see Table 5) and even basic compounds (**32**) may lose the hydrogen bond at this region and thus become less potent. For the flexibility of pyrrolidine, both R and S enantiomers are tolerated in the pocket, but generally the compounds in S configuration can catch hydrogen bonds and fit binding pocket better. Substitutions at position 7 of tetrahydropyrrolopyrimidine are very close to the thiazole

ring, which can change its conformation and affect protein binding. For example, the addition of methyl in 33 significantly drops in activity.

Physical Properties, ADME/PK Profiles of GLS4 and 28a. Compound 28a showed desirable *in vitro* potency and physicochemical properties (Table 6). In the *in vitro* DDI

Table 6. Physical Properties, ADME/PK Profiles

compound ID	GLS4	28a
MW/tPSA	508/76	484/100
CLogP/LogD	4.7/4.4	2.7/2.8
KS (μM)	14	22
liver/plasma ratio of AUC _{0-4h} ($\mu\text{M}\cdot\text{h}$)	9	10
CYP (μM) 1A2/2C9/2C19/2D6/3A4	>50/16/4/52/2	>50/28/39/>50/11
IV (1 mpk)		
$T_{1/2}$ (h)	1.5 \pm 0.1	1.1 \pm 0.1
Vd _{ss} (L/kg)	4.1 \pm 0.6	2.0 \pm 0.2
Cl (mL/min/kg)	56 \pm 7	21 \pm 3
AUC _{0-last} ($\mu\text{M}\cdot\text{h}$)	0.6 \pm 0.1	1.7 \pm 0.2
PO ^{a,b} (10 mpk)		
C_{max} (μM)	0.7 \pm 0.1	4.7 \pm 0.3
AUC _{0-last} ($\mu\text{M}\cdot\text{h}$)	0.8 \pm 0.1	9.1 \pm 1.5
F%	14	54

^aThe single-dose pharmacokinetics of GLS4 and 28a was carried out in female Balb/c mice ($n = 3$) according to standard procedures.

^bVehicle: 1.00 mg/mL in 0.5% HEC.

assessment, compound 28a displayed limited risk on CYP inhibition in a panel of five enzymes (CYP1A2, 2C9, 2C19, 2D6, and 3A4). Compound 28a exhibited moderate plasma clearance (Cl) (21 mL min⁻¹ kg⁻¹) with good oral bioavailability of 54% in mice, while the oral bioavailability of GLS4 was only 14%.

The *in vivo* antiviral activity of 28a was evaluated in a hydrodynamic injection (HDI) HBV mouse model.²⁶ In consideration of higher oral exposure of 28a than GLS4, 28a was dosed at 50 mpk, BID versus GLS4 at 100 mpk, BID. As shown in Figure 2, 28a demonstrated a statistically significant

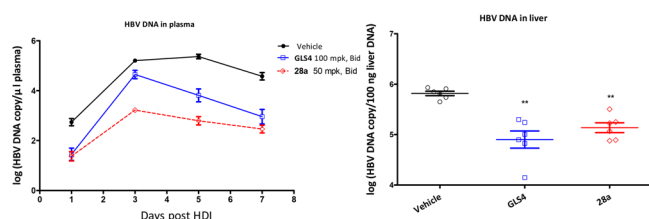


Figure 2. Effect of treatment of GLS4 and 28a on inhibition of HBV replication in HDI mice. Mice ($n = 6$ per group) were orally dosed with vehicle (0.5% HEC), 28a (50 mpk, BID), or GLS4 (100 mpk, BID). The levels of HBV DNA in plasma (A) and liver (B) were determined by qPCR. Error bars represent standard error. Statistical analysis was performed by Student's *t* test. ** $p < 0.01$.

reduction ($p < 0.01$) of HBV DNA in both mouse plasma and liver. In comparison with the vehicle group, 50 mpk (BID) of compound 28a treatment achieved 2.05 and 2.57 log viral DNA reduction in mouse plasma on days 3 and 5, respectively (Figure 2A), while 100 mpk (BID) of reference compound GLS4 treatment achieved 0.35 and 1.56 log viral DNA reduction in mouse plasma on days 3 and 5, respectively. Treatment of the mice with 28a and GLS4 reduced 0.68 and

0.91 log viral load of DNA in mouse liver on day 7, respectively (Figure 2B).

Conclusion. In summary, we have described the successful structural optimization of HAPs to 3,5,6,7-tetrahydropyrrolo-[1,2-*c*]pyrimidines as a novel class of HBV capsid assembly inhibitors. Some of these newly developed derivatives demonstrated highly potent *in vitro* activities against HBV replication. Structural optimization resulted in the identification of one lead compound 28a with an IC₅₀ value of 10 nM in HepG2.2.15 cells. Compound 28a also showed good oral bioavailability with the favorite L/P ratio (10:1) in mice. The HBV HDI mouse model demonstrated that 28a significantly reduced HBV DNA in both mouse plasma and liver. These results demonstrate that 28a is a promising lead compound for further optimization.

■ ASSOCIATED CONTENT

Supporting Information

The Supporting Information is available free of charge on the ACS Publications website at DOI: 10.1021/acsmmedchemlett.7b00288.

Synthetic procedures, analytical data, assay protocol, and inhibitor mechanism of action (PDF)

■ AUTHOR INFORMATION

Corresponding Author

*E-mail: he_haiying@wuxiapptec.com.

Notes

The authors declare no competing financial interest.

■ ABBREVIATIONS

KS, kinetic solubility; PK, pharmacokinetics; L/P ratio, liver/plasma ratio of AUC; SAR, structure–activity relationship; CYP, cytochrome P450; hERG, human ether-a-go-go related gene; IV, intravenous; PO, per oral; AUC, area under curve; mpk, mg/kg

■ REFERENCES

- Yang, X.; Xu, X. A new series of HAPs as anti-HBV agents targeting at capsid assembly. *Bioorg. Med. Chem. Lett.* **2014**, *24*, 4247.
- Liang, T. J. Hepatitis B: The virus and disease. *Hepatology* **2009**, *49*, S13.
- Ferir, G.; Kaptein, S.; Neyts, J. Antiviral treatment of chronic hepatitis B virus infections: the past, the present and the future. *Rev. Med. Virol.* **2008**, *18*, 19.
- Janssen, H. L.; Van-Zonneveld, M.; Senturk, H.; Zeuzem, S.; Akarca, U. S.; Cakaloglu, Y.; Simon, C.; So, T. M.; Gerken, G.; de Man, R. A. Pegylated interferon alfa-2b alone or in combination with lamivudine for HBeAg-positive chronic hepatitis B: a randomised trial. *Lancet* **2005**, *365*, 123.
- Zoulim, F.; Poynard, T.; Degos, F.; Slama, A.; El Hasnaoui, A.; Blin, P.; Mercier, F.; Deny, P.; Landais, P.; Parvaz, P. A prospective study of the evolution of lamivudine resistance mutations in patients with chronic hepatitis B treated with lamivudine. *J. Viral Hepat.* **2006**, *13*, 278.
- Gish, R.; Jia, J.; Locarnini, S.; Zoulim, F. Selection of chronic hepatitis B therapy with high barrier to resistance. *Lancet Infect. Dis.* **2012**, *12*, 341.
- Kim, S. R.; Yang, J.; Kudo, M.; Hino, O. Recent Advances in the Management of Chronic Hepatitis B. *Hepat. Mon.* **2011**, *11*, 601.
- Bang, K. B.; Kim, H. J. Management of antiviral drug resistance in chronic hepatitis B. *World. J. Gastroenterol.* **2014**, *20*, 11641.
- Weber, O.; Schlemmer, K. H.; Hartmann, E.; Hagelschuer, I.; Paessens, A.; Graef, E.; Deres, K.; Goldmann, S.; Niewoehner, U.;

Stoltefuss, J.; Haebich, D.; Ruebsamen-Waigmann, H.; Wohlfeil, S. Inhibition of human hepatitis B virus (HBV) by a novel non-nucleosidic compound in a transgenic mouse model. *Antiviral Res.* **2002**, *28*, 69.

(10) Deres, K.; Schröder, C. H.; Paessens, A.; et al. Inhibition of hepatitis B virus replication by drug-induced depletion of nucleocapsids. *Science* **2003**, *299*, 893.

(11) Bourne, C. R.; Finn, M. G.; Zlotnick, A. Global Structural Changes in Hepatitis B Virus Capsids Induced by the Assembly Effector HAP1. *J. Virol.* **2006**, *80*, 11055.

(12) Stray, S. J.; Zlotnick, A. BAY 41–4109 has multiple effects on Hepatitis B virus capsid assembly. *J. Mol. Recognit.* **2006**, *19*, 542.

(13) Wu, G.; Liu, B.; Zhang, Y.; Li, J.; Arzumanyan, A.; Clayton, M. M.; Schinazi, R. F.; Wang, Z.; Goldmann, S.; Ren, Q.; Zhang, F.; Feitelson, M. A. Preclinical characterization of GLS4, an inhibitor of hepatitis B virus core particle assembly. *Antimicrob. Agents Chemother.* **2013**, *57*, 5344.

(14) Wang, X.; Wei, Z.; Wu, G.; Wang, J.; Zhang, Y.; Li, J.; Zhang, H.; Xie, X.; Wang, X.; Wang, Z.; Wei, L.; Wang, Y.; Chen, H. In vitro inhibition of HBV replication by a novel compound, GLS4, and its efficacy against adefovir-dipivoxil-resistant HBV mutations. *Antiviral Ther.* **2012**, *17*, 793.

(15) Zhou, X.; Gao, Z.; Meng, J.; Chen, X.; Zhong, D. Effects of ketoconazole and rifampicin on the pharmacokinetics of GLS4, a novel anti-hepatitis B virus compound, in dogs. *Acta Pharmacol. Sin.* **2013**, *34*, 1420.

(16) Wang, X.; Wei, Z.; Wu, G.; et al. In vitro inhibition of HBV replication by a novel compound, GLS4, and its efficacy against adefovir-dipivoxil-resistant HBV mutations. *Antiviral Ther.* **2012**, *17*, 793.

(17) Hinkle, G.; Sepp-Lorenzino, L. Hepatitis b virus (hbv) irna compositions and methods of use thereof. WO2016077321A1, 2016.

(18) Slee, H. D.; Chen, Y.; Zhang, X. 2-Amino-N-pyrimidin-4-ylacetamides as A_{2A} Receptor Antagonists: 1. Structure–Activity Relationships and Optimization of Heterocyclic Substituents. *J. Med. Chem.* **2008**, *51*, 1730.

(19) Kappe, C. O. 100 years of the biginelli dihydropyrimidine synthesis. *Tetrahedron* **1993**, *49*, 6937.

(20) The absolute stereochemistry of (–)-enantiomer **20** was determined by its rotation value as reported in WO201437480.

(21) Zlotnick, A.; Venkatakrishnan, B.; Tan, Z.; Lewellyn, E.; Turner, W.; Francis, S. Core Protein: A Pleiotropic Keystone in the HBV Lifecycle. *Antiviral Res.* **2015**, *121*, 82.

(22) Qiu, Z.; Lin, X.; Zhou, M.; Liu, Y.; Zhu, W.; Chen, W.; Zhang, W.; Guo, L.; Liu, H.; Wu, G.; Huang, M.; Jiang, M.; Xu, Z.; Zhou, Z.; Qin, N.; Ren, S.; Qiu, H.; Zhong, S.; Zhang, Y.; Zhang, Y.; Wu, X.; Shi, L.; Shen, F.; Mao, Y.; Zhou, X.; Yang, W.; Wu, J. Z.; Yang, G.; Mayweg, A. V.; Shen, H. C.; Tang, G. Design and Synthesis of Orally Bioavailable 4-Methyl Heteroaryl dihydropyrimidine Based Hepatitis B Virus (HBV) Capsid Inhibitors. *J. Med. Chem.* **2016**, *59*, 7651.

(23) Klumpp, K.; Lam, A. M.; Lukacs, C.; Vogel, R.; Ren, S.; Espiritu, C.; Baydo, R.; Atkins, K.; Abendroth, J.; Liao, G.; Efimov, A.; Hartman, G.; Flores, O. A. High-Resolution Crystal Structure of a Hepatitis B Virus Replication Inhibitor Bound to the Viral Core Protein. *Proc. Natl. Acad. Sci. U. S. A.* **2015**, *112*, 15196.

(24) *The PyMOL Molecular Graphics System*, version 1.8; Schrödinger, LLC: New York

(25) *Schrödinger Release 2017–2: Maestro*; Schrödinger, LLC: New York, 2017.

(26) Huang, L. R.; Gabel, Y. A.; Graf, S.; Arzberger, S.; Kurts, C.; Heikenwalder, M.; Knolle, P. A.; Protzer, U. Transfer of HBV genomes using low doses of adenovirus vectors leads to persistent infection in immune competent mice. *Gastroenterology* **2012**, *142*, 1447.